Sun *Energy Informatics* (2024) 7:30
https://doi.org/10.1186/s42162-024-00332-4

Energy Informatics

RESEARCH Open Access

Self-operation and low-carbon scheduling optimization of solar thermal power plants with thermal storage systems

Jing Sun[1*]

*Correspondence:
Sunjing0909_2000@126.com

[1] Department of Mechanical and Electrical Engineering, Ordos Vocational College of Eco-Environment, Ordos 017000, China

Abstract

Photo thermal power generation, as a renewable energy technology, has broad development prospects. However, the operation and scheduling of photo thermal power plants rarely consider their internal structure and energy flow characteristics. Therefore, this study explains the structure of a solar thermal power plant with a thermal storage system and analyzes its main energy flow modes to establish a self-operation and low-carbon scheduling optimization model for the solar thermal power plant. The simulation results of the example showed that for the self-operating model oriented towards power generation planning and peak valley electricity prices, the existence of a thermal storage system could improve the power generation capacity and revenue of the photovoltaic power plant. For example, when the capacity of the thermal storage system was greater than 6 h, the penalty for insufficient power generation in the simulation result was 0 $, and the maximum increase in revenue reached 84.9% as the capacity of the thermal storage system increased. In addition, when the capacity of the thermal storage system increased from 0 to 8 h, the comprehensive operating cost decreased from 1635.2 k $ to 1224.6 k $, and the carbon emissions decreased from 26.4×10^3 ton to 22.1×10^3 ton. Compared with the existing literature, this study provides a more comprehensive and systematic solution through detailed energy flow analysis and optimization model. The research has practical and far-reaching significance for promoting the development of clean energy technology, improving the sustainable utilization of renewable energy, and optimizing the overall performance of the energy system.

Keywords: Renewable energy technology, Thermal storage system, Photo thermal power plant, Self operation, Low carbon scheduling

Introduction

Under the dual pressures of the global energy crisis and climate change, seeking sustainable and low-carbon energy solutions has become a common challenge for scientists, engineers, and policymakers (Carley and Konisky 2020). Due to the fact that solar energy is a rich and clean energy resource, photo thermal power plants (PTPPs) have received widespread attention for their efficient conversion of solar radiation into electrical energy (Wang et al. 2021). Photo thermal power generation (PPG), also known as

concentrated solar power generation, is an emerging large-scale solar power generation technology that follows photovoltaic power generation. The difference between PPG principle and conventional thermal power lies in the source of thermal energy. Conventional thermal power uses fossil fuels for combustion to generate thermal energy, while PPG, with the help of a focusing mirror, gathers sunlight into a collector, which then converts solar radiation into thermal energy (Haruna et al. 2023). Traditional photovoltaic power plants (PVPP) utilize the photovoltaic effect of semiconductor materials to convert solar energy into electrical energy. However, the output of PVPP is unstable due to the interference of meteorological factors such as day night alternation and rainy weather during its operation (Manoharan et al. 2020). In addition, generally speaking, the output of PVPP is concentrated at noon, while the electricity demand reaches its maximum in the evening, so the two cannot be matched and will have an impact on the safety and economy of the power system operation (Frizzo Stefenon et al. 2020). PTPP with thermal storage system (TSS) has certain scheduling ability, and its thermal system can smooth out the fluctuation of solar radiation power. At the same time, the presence of TSS can store thermal energy, which is beneficial for PTPP night power generation (Hou et al. 2021). Compared to PVPP, PTPP is more suitable for large-scale power generation and grid connection. Palacios et al. (2020) reviewed the current state and future trends of PPG, noting that PPG can provide supplemental energy and dispatchable power on demand through the use of integrated thermal energy storage systems, and argued that PPG's main efforts must focus on improving its ability to transfer heat demand over days, weeks, or even months. However, the structure of PTPP components is complex and diverse, and the power generation process involves multiple links. Its operation scheduling needs to consider many issues, including energy coupling relationships (Shakya 2021). Therefore, this study starts with the basic structure of PTPP, focuses on the internal energy flow characteristics (IEFCs) of PTPP, and establishes a PTPP self-operation and low-carbon scheduling optimization (LCSO) model. This study aims to improve the automation, adaptability, and low-carbon performance of PTPP, improve its scheduling mode, and make positive contributions to the development of sustainable energy systems, laying the foundation for building a cleaner and more sustainable energy future.

The content has four parts. Part 1 introduces the current research on PPG, PTPP, and other related topics worldwide. Part 2 establishes a self-operating and LCSO model based on the internal structure of PTPP. Part 3 conducts numerical analysis on the proposed self-running LCSO model to verify its effectiveness. Part 4 provides a comprehensive summary and analysis of the paper.

Related work

PPG is a technology that utilizes solar energy to generate electricity, which has many advantages in renewable energy and environmental protection. For example, using solar energy as an energy source can help reduce dependence on limited resources while reducing negative impacts on the environment. Therefore, many scholars around the world have conducted extensive research on PPG related content. Schöniger et al. (2021) compared the technology configurations of photovoltaic power generation and PPG combined with TES to address the issue that solar energy can only be used during sunny days. Through simulation without

sunlight, it was found that PPG combined with TES can effectively improve energy storage time, providing a new solution for solving solar energy usage limitations. Yousef et al. (2021) explored the latest developments in PPG and various energy integration technologies in response to the rapid development of PPG. The combination of PPG and fossil fuels could more effectively cope with the intermittency of solar energy compared to individual PPG, and could effectively reduce the cost of PTPP and increase power generation. Buendía Martínez et al. (2020) proposed a high-precision measurement scheme for focusing mirrors in PPG, which effectively improves the efficiency and power generation of PPG by improving instrument accuracy. Hamilton et al. (2020) proposed a scheme that combines PPG systems with photovoltaic power generation systems and TES to address the cost issue of PPG. They also designed an evaluation model for hybrid systems, providing effective information for the design practice of hybrid power systems and reducing power generation costs.

PTPP is a facility that utilizes solar energy for electricity generation. It converts solar radiation into thermal energy by focusing on sunlight, and then uses the thermal energy to generate steam, ultimately driving a generator to generate electricity. The advantages of PTPP include renewable energy utilization, low carbon emissions, sustained performance, and multifunctional applications. Therefore, a large number of scholars are attracted to conduct research on it. Kunwer et al. (2022) proposed an integrated TES and PPG scheme to address the issue of intermittent solar energy leading to high power costs in PPG, effectively reducing the average power output cost of PTPP and providing a better profit model. Khaloie et al. (2021) proposed a PTPP day ahead and day ahead scheduling model with a two-stage stochastic structure to address issues such as uncertainty and decision sequence in the electricity market. It used information gap decision-making theory to handle uncertainty related to solar energy, effectively optimizing the operating mode of PTPP. Fang et al. (2021) proposed a complementary solution using wind farms and PTPP to address the issue of frequent adjustments in real-time power output caused by unreasonable market design. It further proposed adjusting the optimal bidding strategy, thereby effectively improving the durability and profitability of PTPP. Yu et al. (2020) proposed a scenario based stochastic framework for optimizing PTPP scheduling in response to the uncertainty of solar irradiance and electricity market prices faced by PTPP. This framework could obtain the optimal selling curve, thereby selling electricity to the electricity market and increasing expected profits.

In summary, there are optimization problems in the operation and scheduling of PTPP currently, including but not limited to cost optimization, power generation optimization, etc. In addition, in the research of many scholars, there is almost no involvement in the internal structural components and complex energy coupling relationship of PTPP. Therefore, this study proposes a PTPP self-running LCSO model that considers IEFCs. This study comprehensively considers the technical and economic characteristics of each module of PTPP, as well as the nonlinear characteristics of the thermoelectric efficiency of the power generation module, which is innovative.

Establishment of LCSO model for PTPP self-transport containing TSS

This section analyzes the basic structure of PTPP, establishes a PTPP self-operating model, and based on the operating model, establishes an LCSO model for power systems containing PTPP with the goal of minimizing fuel cost, carbon emission cost, and power shortage penalty.

Internal structure and energy flow analysis of PTPP

At present, conventional power plant operation models cannot accurately characterize the energy flow characteristics of power plants such as PTPP. Therefore, before constructing the PTPP operation model, it is necessary to analyze the IEFCs of PTPP. The energy flow characteristics are closely related to the internal basic structure of PTPP. PTPP contains relatively independent energy modules. According to their different functions, the energy modules are divided into three categories: Solar Field (SF), TES, and Power Block (PB). In addition, PTPP also includes an energy transfer system called the Heat Transfer System (HTS) (Ding and Bauer 2021). The internal structure of PTPP, which refers to the relationship between various modules, is shown in Fig. 1.

In Fig. 1, the heat exchange between the SF, TES, and PB modules relies on the cyclic flow of the thermal conductive medium in HTS. SF focuses solar radiation onto the collector through a focusing mirror, converts solar energy into thermal energy, and stores it in a thermal conductive medium. The thermal conductive medium can flow directly to PB or to TES. In PB, the heat exchanger transfers heat energy to high-temperature and high-pressure steam, which is then supplied to the power plant through the turbine and generator. TES can store thermal conductive media and transfer them to PB even when solar energy is not available. Therefore, based on the analysis of the basic internal structure of heating electrons, this study obtained their internal energy flow process, as shown in Fig. 2.

In Fig. 2, the solar radiation power P^{DNI} is converted by SF to output thermal power P^{sf} to the thermal medium. P^{sf} can be further divided into heat storage power P^{chg} flowing towards TES and power generation power P^{pb} flowing towards PB. The energy in TES flows towards PB in the form of exothermic power P^{dsg}, and ultimately PB outputs electricity

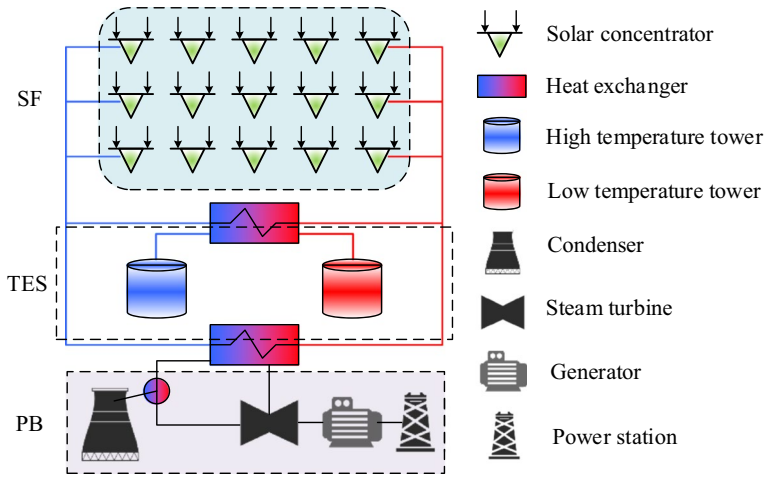

Fig. 1 Schematic diagram of the internal structure of the PTPP

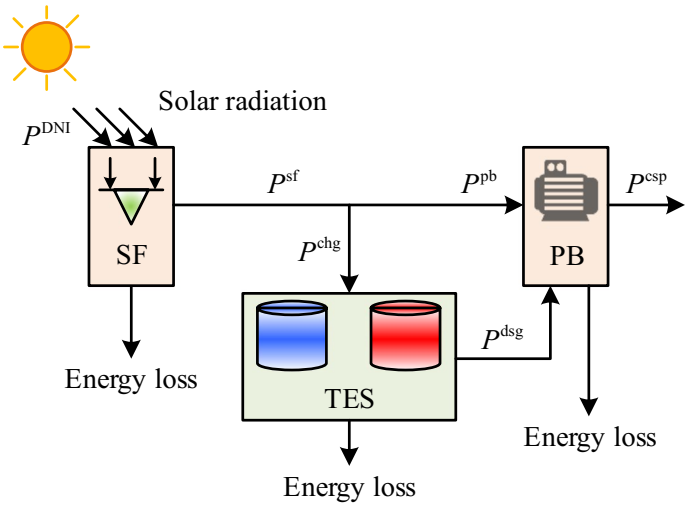

Fig. 2 Diagram of energy flow inside the PTPP

P^{csp}. In addition, all three modules experience a certain proportion of energy loss during energy storage, transfer, and other processes.

In the actual operation process of a heating power plant, each module has different working states. Therefore, this study divides the energy flow modes of thermal power plants into six categories, namely, heat collection–heat storage (M1), heat collection–heat storage–power generation (M2), heat collection–power generation (M3), heat collection–heat releasing–power generation (M4), heat releasing–power generation (M5), and all idle (M6) modes. M1 usually occurs in the early morning when the solar radiation is low, and all the energy from the SF module flows into the TES, leaving the power generation module idle (Bloomfield et al. 2021). M2 generally appears during noon when the solar radiation is high, with some of the energy from SF flowing into TES and some flowing into PB. M3 generally receives all the energy from SF flowing into PB around noon when the solar radiation is moderate. In the evening, it is usually M4, while in the evening peak hours, it is M5, while M6 is used for nighttime and cloudy days. In practice, PTPP can flexibly switch these modes to achieve efficient power generation operation based on changes in solar radiation and grid demand.

PTPP self-running model and objective function construction

This study constructs corresponding operational models for three modules. Firstly, an expression for the total solar radiation power of PTPP during period t is established, as shown in Eq. (1).

$$P_t^{\mathrm{DNI}} = A_{\mathrm{sf}} x_t^{\mathrm{DNI}}. \tag{1}$$

In Eq. (1), A_{sf} represents the field area of the spotlight mirror in SF. x_t^{DNI} represents the normal direct solar radiation intensity during period t. The available thermal power P_t^{solar} of SF during period t is Eq. (2).

$$P_t^{\mathrm{solar}} = \eta_{\mathrm{m}} \eta_{\mathrm{r}} P_t^{\mathrm{DNI}} = \eta_{\mathrm{sf}} P_t^{\mathrm{DNI}}. \tag{2}$$

In Eq. (2), η_{m} represents the mirror reflection efficiency. η_{r} represents the conversion efficiency of the receiver. η_{sf} represents the comprehensive photo thermal efficiency of the SF module. The output thermal power P_t^{sf} of SF is generally the same as the available thermal power value. However, considering that when the solar radiation intensity is too high, SF will lose some energy. Therefore, in this study, heat rejection power is added to the output thermal power of SF, as shown in Eq. (3).

$$P_t^{\mathrm{sf}} = P_t^{\mathrm{solar}} - P_t^{\mathrm{CoS}}. \tag{3}$$

In Eq. (3), P_t^{CoS} represents the heating power during period t. The thermal storage level E_t of TES during period t involves multiple factors, including thermal storage power P_t^{chg}, heat release power P_t^{dsg}, and the previous thermal storage level E_{t-1}. The energy balance equation of TES is Eq. (4).

$$E_t = (1-\eta_{\mathrm{e}})E_{t-1} + \left(\eta_{\mathrm{c}} P_t^{\mathrm{chg}} - \frac{P_t^{\mathrm{dsg}}}{\eta_{\mathrm{d}}}\right)\Delta t. \tag{4}$$

In Eq. (4), η_{e} represents the heat dissipation coefficient of TES during time interval Δt. η_{c} and η_{d} represent the thermal storage efficiency and heat release efficiency of TES, respectively. The upper limit of heat transfer rate will constrain the thermal storage power and heat release power of TES as shown in Eq. (5).

$$\begin{cases} 0 \le P_t^{\mathrm{chg}} \le y_t^{\mathrm{chg}} \cdot P_{\max}^{\mathrm{chg}} \\ 0 \le P_t^{\mathrm{dsg}} \le y_t^{\mathrm{dsg}} \cdot P_{\max}^{\mathrm{dsg}} \end{cases}. \tag{5}$$

In Eq. (5), y_t^{chg} and $P_{\max}^{\mathrm{chg}}$ represent the binary auxiliary variables of thermal storage and the maximum thermal storage power, respectively. y_t^{dsg} and $P_{\max}^{\mathrm{dsg}}$ represent binary auxiliary variables for heat release and maximum heat release power, respectively. The working state of TES (heat storage, heat release, idle) is constrained by the single flow characteristic of the medium, as shown in Eq. (6).

$$y_t^{\mathrm{chg}} + y_t^{\mathrm{dsg}} \le 1. \tag{6}$$

The way PB converts thermal energy into electrical energy is through the steam cycle, and its thermal power balance equation is Eq. (7).

$$P_t^{\mathrm{pb}} = P_t^{\mathrm{ST}} + r_t^{\mathrm{pb}} P_{\mathrm{SU}}^{\mathrm{pb}}. \tag{7}$$

In Eq. (7), P_t^{pb} represents the thermal power of PB during period t. P_t^{ST} represents the thermal power used for power generation during period t. $P_{\mathrm{SU}}^{\mathrm{pb}}$ represents the thermal power consumption of PB. r_t^{pb} represents a binary auxiliary variable. The constraints of PB are relatively complex, including logical relationship constraints, hotspot conversion efficiency constraints, and operational constraints, as shown in Table 1.

In Table 1, u_t^{pb} and u_{t-1}^{pb} represent the binary variables of PB startup and shutdown status in time periods t and $t-1$, respectively. When their values are 1, they indicate startup, and vice versa, they indicate shutdown. P_t^{csp} represents the power output of

Table 1 Constraint formula table of PB module

Constraint condition	Constrained branch	Equation
Non-run constraint	Logical relation constraint	$u_t^{\mathrm{pb}} - u_{t-1}^{\mathrm{pb}} \le r_t^{\mathrm{pb}} \le \frac{\left(1+u_t^{\mathrm{pb}}-u_{t-1}^{\mathrm{pb}}\right)}{2}$
	Efficiency constraints of thermoelectric conversion	$P_t^{\mathrm{csp}} = \eta_{\mathrm{pb}} P_t^{\mathrm{ST}}$
Run constraint	Maximum and minimum output constraints	$u_t^{\mathrm{pb}} P_{\min}^{\mathrm{csp}} \le P_t^{\mathrm{csp}} \le u_t^{\mathrm{pb}} P_{\max}^{\mathrm{csp}}$
	Climb up and down constraints	$-R_{\mathrm{down}}^{\mathrm{csp}} \Delta t \le P_t^{\mathrm{csp}} - P_{t-1}^{\mathrm{csp}} \le R_{\mathrm{up}}^{\mathrm{csp}} \Delta t$
	Minimum boot time constraint	$\sum_{\tau=t-T_{\mathrm{on}}^{\mathrm{pb}}}^{t-1} u_\tau^{\mathrm{pb}} \ge T_{\mathrm{on}}^{\mathrm{pb}} \left(u_{t-1}^{\mathrm{pb}} - u_t^{\mathrm{pb}}\right)$
	Minimum downtime constraints	$\sum_{\tau=t-T_{\mathrm{off}}^{\mathrm{pb}}}^{t-1} \left(1 - u_\tau^{\mathrm{pb}}\right) \ge T_{\mathrm{off}}^{\mathrm{pb}} \left(u_t^{\mathrm{pb}} - u_{t-1}^{\mathrm{pb}}\right)$

PTPP during period t. η_{pb} represents the thermal efficiency of PB. $P_{\min}^{\mathrm{csp}}$ and $P_{\max}^{\mathrm{csp}}$ represent the minimum and maximum technical output of the PB generator set, respectively. $R_{\mathrm{down}}^{\mathrm{csp}}$ and $R_{\mathrm{up}}^{\mathrm{csp}}$ represent the downhill and uphill rates of the generator set, respectively. $T_{\mathrm{on}}^{\mathrm{pb}}$ and $T_{\mathrm{off}}^{\mathrm{pb}}$ respectively represent the minimum startup and shutdown time of PB. The logical relation constraint ensures the consistency of the startup and shutdown states of PB module. The efficiency constraint of thermoelectric conversion ensures that the process of converting thermal energy into electrical energy conforms to the technical parameters. Operational constraints cover the limitations of PB modules in actual operation, such as upper and lower limits of output power and thermal power consumption, to maintain safety and efficiency. The maximum and minimum output constraints define the power output range of the PB module to balance supply and demand and keep the grid stable. Climb and descent constraints limit the rate at which PB modules can adjust output power to prevent equipment damage or grid instability. Minimum startup time and downtime constraints specify the minimum time required for PB modules to start and shut down, reducing wear and tear on equipment caused by frequent startup and shutdown. The thermal power exchange between the three modules of PTPP conforms to the law of energy conservation, as shown in Eq. (8).

$$P_t^{\mathrm{sf}} + P_t^{\mathrm{dsg}} = P_t^{\mathrm{chg}} + P_t^{\mathrm{pb}}. \tag{8}$$

This study establishes two PTPP self-operating objectives. The first goal is aimed at the power generation plan, which means that after receiving the power generation plan formulated by the power grid dispatch center, PTPP will adjust its own operating strategy. The objective function is Eq. (9).

$$\begin{cases} \min F^{\mathrm{sche}} = \sum_{t=1}^{T} \pi_t^{\mathrm{vio}} \Delta P_t^{\mathrm{vio}} \Delta t \\ \Delta P_t^{\mathrm{vio}} = \begin{cases} P_t^{\mathrm{sche}} - P_t^{\mathrm{csp}}, P_t^{\mathrm{csp}} < P_t^{\mathrm{sche}} \\ 0, P_t^{\mathrm{csp}} > P_t^{\mathrm{sche}} \end{cases} \end{cases}. \tag{9}$$

In Eq. (9), F^{sche} represents the penalty for violating the power generation plan. π_t^{vio} represents the penalty factor for violating the power generation plan during period t. ΔP_t^{vio} represents the number of violations during period t. P_t^{sche} represents the planned power generation output during the t period. The second goal is to establish a peak valley electricity pricing mechanism for the electricity market. Due to the presence of TSS, PTPP power generation has adjustable ability, so the objective function is Eq. (10).

$$\max F^{\text{pric}} = \sum_{t=1}^{T} \pi_t^{\text{pric}} P_t^{\text{csp}}. \tag{10}$$

In Eq. (10), F^{pric} represents the revenue of PTPP. π_t^{pric} represents the electricity price during period t.

PTPP power system LCSO model

When scheduling the PTPP power system, due to the electricity efficiency and carbon reduction benefits of PPG, it is necessary to consider scheduling cost factors including fuel cost and carbon emission cost (Guerra et al. 2020). The objective of the PTPP power system LCSO model constructed in this study is to ensure the lowest operating cost F^{oper}, as shown in Eq. (11).

$$\min F^{\text{oper}} = F^{\text{fuel}} + F^{\text{carb}} + F^{\text{curL}} + F^{\text{curS}}. \tag{11}$$

In Eq. (11), F^{fuel} represents fuel cost. F^{carb} represents the cost of carbon emissions. F^{curL} represents the penalty cost for load shedding. F^{curS} represents the penalty fee for insufficient backup. The expression of F^{fuel} is Eq. (12).

$$F^{\text{fuel}} = \sum_{i=1}^{N} \sum_{t=1}^{T} \left[C_i^{\text{fuel}} \cdot f^{\text{fuel}}\left(P_{i,t}^{\text{thm}}\right) + r_{i,t} SU_i \right]. \tag{12}$$

In Eq. (12), N represents the total number of conventional units. C_i^{fuel} represents the unit fuel cost of Unit i. $P_{i,t}^{\text{thm}}$ represents the output of the i-th unit during period t. $f^{\text{fuel}}\left(P_{i,t}\right)$ represents the fuel consumption of the i-th unit during period t. $r_{i,t}$ represents a binary auxiliary variable. SU_i represents the start-up cost of the i-th unit. The variables included in this formula represent economic considerations in LCSO, and the aim is to optimize these parameters to minimize operating costs while ensuring the stability of the power supply and meeting environmental standards. The definition of F^{carb} is Eq. (13).

$$F^{\text{carb}} = \sum_{i=1}^{N} \sum_{t=1}^{T} \left\{ C^{\text{carb}} \left[K_i^{\text{fuel}} \cdot f^{\text{fuel}}\left(P_{i,t}^{\text{thm}}\right) + r_{i,t} SE_i \right] \right\}. \tag{13}$$

In Eq. (13), C^{carb} represents the cost of carbon dioxide emissions. K_i^{fuel} represents the carbon emission coefficient per unit fuel of the i-th unit. SE_i represents the starting carbon emissions of the i-th unit. In practice, PTPP needs to calculate its carbon emission cost based on the fuel consumption and carbon emission coefficient of each unit, and incorporate these costs into the total cost for optimal scheduling to reduce the impact on the environment. The expression of F^{curL} and F^{curS} is Eq. (14).

$$\begin{cases} F^{\mathrm{curL}} = \sum_{t=1}^{T} C^{\mathrm{curL}} P_t^{\mathrm{curL}} \Delta t \\ F^{\mathrm{curS}} = \sum_{t=1}^{T} C^{\mathrm{curS}} P_t^{\mathrm{curS}} \Delta t \end{cases}. \tag{14}$$

In Eq. (14), C^{curL} and C^{curS} represent the penalty coefficients for load shedding and insufficient backup, respectively. P_t^{curL} and P_t^{curS} respectively represent the load shedding and insufficient backup during period t. The secondary consumption characteristic curve of conventional units is Eq. (15).

$$f^{\mathrm{fuel}}\left(P_{i,t}^{\mathrm{thm}}\right) = a_i\left(P_{i,t} \times P_{i,t}\right) + b_i P_{i,t} + c_i u_{i,t}. \tag{15}$$

In Eq. (15), a_i, b_i, and c_i respectively represent the secondary consumption coefficients of the i-th unit. $u_{i,t}$ is a binary variable representing the start and stop status of the i-th unit during the t period. In practical applications, the power station scheduler needs to consider these nonlinear characteristics to optimize the operation strategy of the unit, better arrange the start-up, operation and shutdown of the unit, adapt to the changes of the power grid load, and reduce unnecessary energy waste, so as to improve the overall operation efficiency and reduce costs. The constraints of the LCSO model involve a wide range, as shown in Fig. 3.

In Fig. 3, j/w, $N^{\mathrm{csp}}/N^{\mathrm{wind}}$, and $P_{j,t}^{\mathrm{csp}}/P_{w,t}^{\mathrm{wind}}$ represent the index, total number, and output of PTPP and wind farms. P_t^{loadF} and R_t^{gridS} represent the load demand and rotational reserve capacity of the power grid during the t period. $R_{j,t}^{\mathrm{cspS}}$ and $R_{i,t}^{\mathrm{thmS}}$ represent the rotational reserve capacity of the jth and ith PTPP units during period t. $P_{\mathrm{min},i}^{\mathrm{thm}}$ and $P_{\mathrm{max},i}^{\mathrm{thm}}$ represent the maximum and minimum output of the i-th unit, respectively. $R_{\mathrm{down,i}}^{\mathrm{thm}}$ and $R_{\mathrm{up,i}}^{\mathrm{thm}}$ respectively represent the maximum uphill and downhill speeds of the i-th unit. $T_{\mathrm{on,i}}^{\mathrm{thm}}$ and $T_{\mathrm{off}}^{\mathrm{thm}}$ respectively represent the minimum start-up and shutdown time of the i-th unit. $P_{w,t}^{\mathrm{curW}}$ and $P_{w,t}^{\mathrm{windF}}$ respectively represent the maximum generated output and

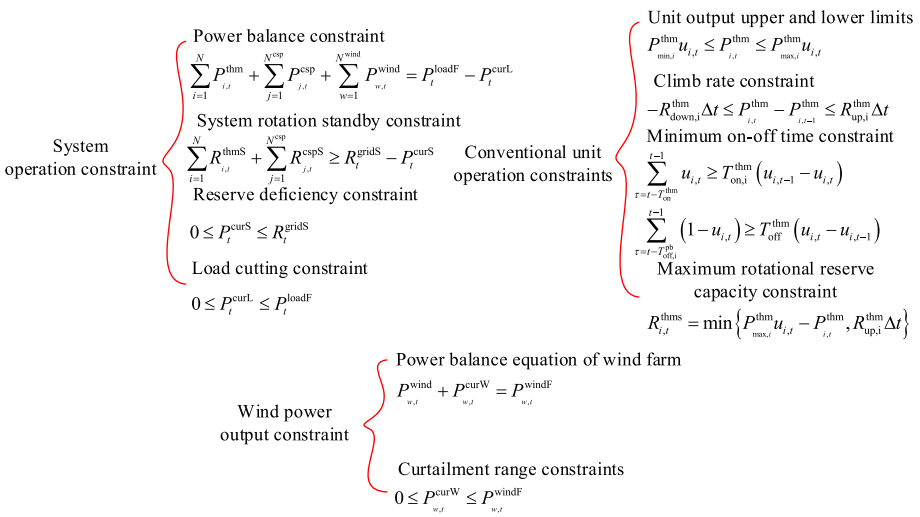

Fig. 3 The constraints of the low-carbon scheduling optimization model

abandoned wind power of wind power during the t period. Both the LCSO model proposed in this study and the work of Schöniger et al. (2021) focused on the economic benefits of PPG, especially in combination with the configuration of TES. However, this study provides a more accurate scheduling strategy by deeply analyzing the internal energy flow of PTPP, establishing a detailed optimization model, and considering the nonlinear characteristics of thermoelectric efficiency.

Case analysis of PTPP self-running LCSO model

To verify the effectiveness of the constructed self-operated LCSO model, this study conducts extensive simulation calculations to analyze the impact of thermal storage modules on the self-operation of PTPP, as well as the impact of module capacity and light field capacity on the low-carbon scheduling of the system.

Construction of simulation example experimental environment and data setting

The hardware platform for simulation computing is a workstation equipped with two Intel Xeon E5-2680 (2.4 GHz) processors and 128 GB RAM. The software environment for simulation calculation includes Windows 7 64 bit operating system, MATLAB programming environment, YALMIP toolbox, and GUROBI solver. The technical parameter data of the simulated time-thermal power station are mainly from the empirical parameters of the trough photothermal power station model in the SAM software developed by NREL, and the parameters are determined based on technical feasibility, economy, environmental impact and policy requirements. These parameters are sensitive to the results, such as TES capacity affecting nighttime power generation capacity, photo thermal conversion efficiency affecting energy utilization rate. Operating costs and electricity prices affect revenue, while carbon costs are related to environmental compliance. The specific data are shown in Table 2.

In addition to the technical parameter settings in Table 2, this study conducted different simulation settings for PTPP self-operation and LCSO. There are two scenarios for self-running simulation design, one is suitable for the power grid with evening peak load (Scenario A), and the other is suitable for the power grid with afternoon peak load (Scenario B). In Scenario A, PTPP relies on a heat storage system to release the heat stored during the day to meet the electricity demand during peak hours. It is expected that this scenario will demonstrate the ability of PTPP to maintain efficient power generation through TES in the absence of sunlight. Scenario B is designed to test the maximum power generation potential of PTPP under direct sunlight and how

Table 2 Technical parameters of the simulated PTPP

Parameter type	Value	Parameter type	Value
Rated generating capacity	110.00 MW	Solar multiple	1.50
Maximum technical capacity	115.00 MW	Capacity of the TES	4.20 h
Minimum technical output	35.00 MW	Light-heat conversion efficiency	80.00%
Minimum downtime	2.30 h	Heat storage and release efficiency	97.80%
Climbing speed	85.00 MW/h	Hourly heat storage loss	0.03%
Start-up thermal power loss	60.30 MW	Thermoelectric conversion efficiency	31.35%-38.53%

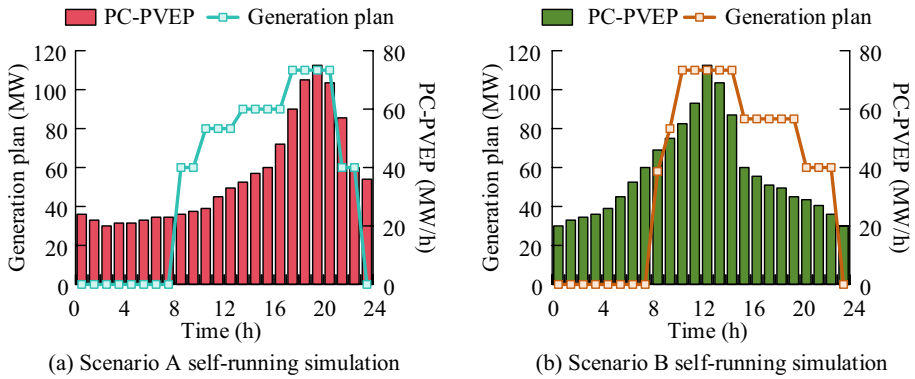

Fig. 4 Self-running simulation scenario

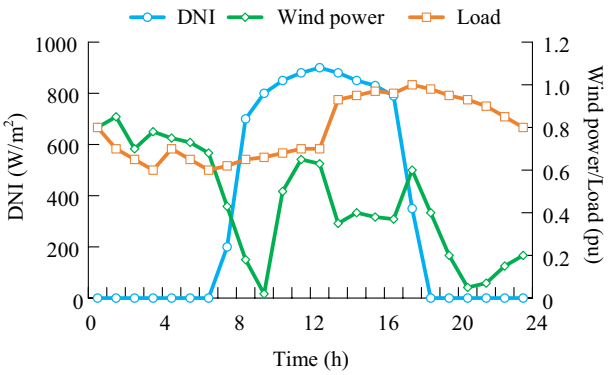

Fig. 5 Simulation of low-carbon scheduling optimization

efficiently solar energy can be utilized and converted during peak hours. This scenario is expected to demonstrate the power generation efficiency of PTPP under conditions of high solar radiation, as well as the strategies of TES in balancing supply and demand and storing excess energy. The daytime and nighttime peak load periods are the moments when the grid demand fluctuates the most, and the setting of scenario A and Scenario B can comprehensively evaluate the performance of the model. This setting can not only reflect the actual power demand mode, verify the energy storage capacity of solar thermal power station technology under the condition of no sunlight and the power generation efficiency under the strong solar radiation, but also help to optimize the scheduling strategy and provide data support for policy making. LCSO simulation is an improvement on the IEEE-RTS-96 system. The self-running simulation scenario is Fig. 4.

In Fig. 4, PC-PVEP represents the penalty coefficient peak valley electricity price. In Fig. 4a, in scenario A, both the PC-PVEP and the power generation plan reach their maximum values during the 18–20 h period, at 115 MW/h and 75WM, respectively. In Fig. 4b, in scenario B, both PC-PVEP and power generation plan reach their maximum values during the 10–14 h period, which are also 115 MW/h and 75WM, respectively. The load, wind power output, and Direct Normal Irradiance (DNI) curves in LCSO simulation are shown in Fig. 5.

In Fig. 5, the wind power simulation value is the lowest at 10 h, which is 0.02 pu. The predicted load value before 12 h is lower than the value after 12 h, and the DNI reaches its maximum at noon. The simulation curve set for this study is in line with the vast majority of practical situations in reality.

Analysis of PTPP self-operation results

This study names the two self-operating objectives of PTPP, namely the peak and valley electricity pricing mechanism for power generation planning and the electricity market, as Goal I and Goal II, respectively. Then, the two are named Scheme AI and AII respectively when running in the self-running simulation scenario A. Run under scenario B of the self-running simulation, named scheme BI and BII respectively. This study analyzes the internal thermal power balance of PTPP for four schemes. Firstly, the Goal I is analyzed, as shown in Fig. 6.

According to Fig. 6a, Scheme AI exhibited a phenomenon of thermal power discard during the period from 14 to 16 h, indicating that the generation of thermal energy exceeded demand. During the period from 22 to 24 h, it showed a deficiency in thermal power, suggesting that the thermal energy storage system failed to meet the nighttime heat demand. As shown in Fig. 6b, Scheme BI's thermal energy management performed well, with virtually no thermal power discard, demonstrating the effectiveness of its thermal energy storage system capacity and heat release strategy. Figure 6c indicates that the thermal power station of Scheme AII utilizes the thermal energy storage module to store heat during the daytime, and starting from 6 pm, the thermal storage module begins

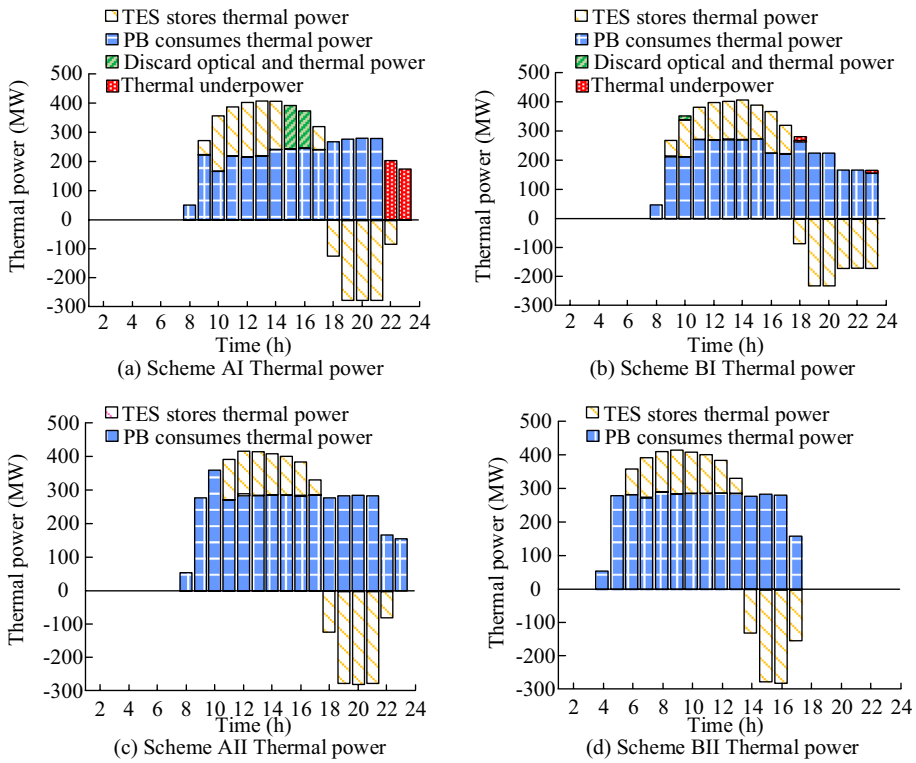

Fig. 6 Internal thermal power balance of the photo thermal plant under target I

to release heat to meet the nighttime heat demand. Figure 6d reveals that the thermal power station of Scheme BII opts to store thermal energy during the morning hours, and from 2 pm onwards, the thermal storage module starts to release heat to address the peak thermal energy demand in the afternoon to evening period. Furthermore, the influence of TSS capacity on the self-operation of PTPP is studied and discussed, and the results are shown in Fig. 7.

As the TSS capacity (the time it can store heat) increases, the penalty for insufficient power generation (IPDP) in schemes AI and BI decreases. Specifically, when the TSS capacity is 0 h, the IPGP of AI and BI are 31,577 $ and 9213 $, respectively. When the TSS capacity is 6 h, the IPGP of AI is 0 $, and when the TSS capacity is 5 h, the IPGP of scheme BI is 0 $. In addition, solar energy resources are relatively abundant during noon hours, and the matching between scenario B and solar energy resources is better than scenario A, so the penalty for scenario BI is lower. Increasing TSS capacity can have a positive impact on the generation revenue of AII and BII solutions. As the capacity of the thermal storage module increases from 0 to 6 h, the power generation revenue of scheme AII increases from $34,830 to $64,409, an increase of 84.9%. Similarly, under the BII scheme, the power generation revenue increased by 15.3% from $54,240 to $62,251.9.

Analysis of low-carbon scheduling results for PTPP

This study analyzes the low-carbon scheduling results of PTPP from multiple perspectives. Firstly, some technical and economic indicators of scheduling were compared under different TSS capacities, and the results are shown in Table 3.

In Table 3, when the TSS capacity increases from 0 to 8 h, the comprehensive operating cost decreases from 1635.2 k $ to 1224.6 k $, and the carbon emissions decrease from 26.4×10^3 ton to 22.1×10^3 ton. This is because the existence of TSS can utilize the solar energy stored during the day to generate electricity at night, reducing costs and carbon emissions. However, when the TSS capacity increases from 4 to 8 h, indicators including comprehensive operating costs remain almost unchanged or undergo slight changes. This is because the capacity of 4 h TSS is sufficient to solve the problem of abandoned light, and increasing the TSS capacity no

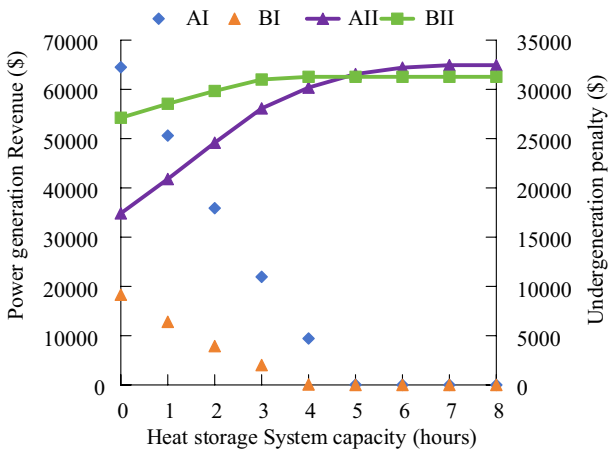

Fig. 7 Self-operation results of heating power station

Table 3 Comparison of dispatching technical and economic indicators

Capacity (h)	0	2	4	6	8
Comprehensive operating cost (k$)	1635.2	1312.8	1233.8	1232.6	1224.6
Generation cost (k$)	704.0	677.7	652.3	650.8	650.4
Start-stop cost (k$)	75.1	50.6	25.8	25.8	25.8
Carbon emissions (10^3ton)	26.4	25.2	22.4	22.3	22.1
Shear load (MWh)	117.4	0.0	0.0	0.0	0.0
Insufficient reserve (MWh)	122.3	0.0	0.0	0.0	0.0
Wind power (MWh)	923.8	948.7	948.7	948.7	948.7
Discarded light power (MWh)	1974.4	934.8	0.0	0.0	0.0

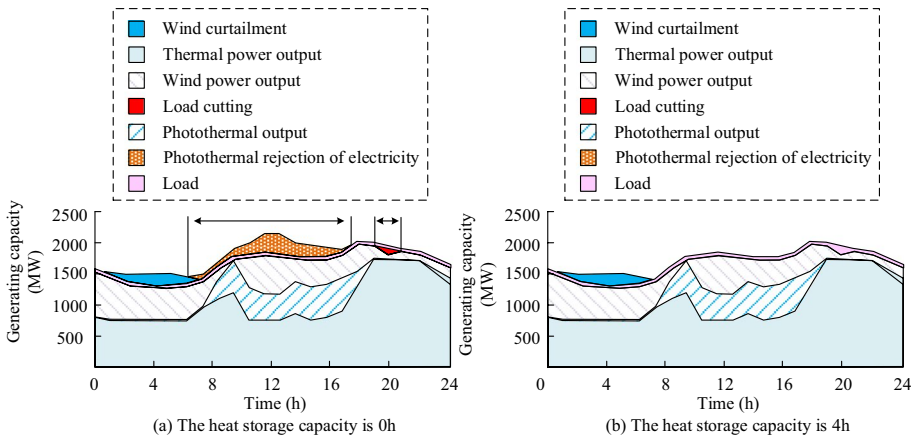

Fig. 8 PTPP scheduling plan

longer significantly increases the power generation of PTPP. The scheduling plan of PTPP at TSS capacities of 0 h and 4 h is Fig. 8.

In Fig. 8a, when the TSS capacity is 0 h, there is no TSS, and a large amount of abandoned light occurs during the 7–17 h time period. In addition, at 20 h at night, due to zero solar radiation, PTPP is unable to generate electricity, resulting in system load shedding. In Fig. 8b, when the TSS capacity is 4 h, PTPP avoids the phenomenon of light curtailment and can continue to generate electricity during peak hours at night, avoiding system load shedding. Finally, this study investigates the impact of solar multiple changes on PTPP scheduling results, as shown in Fig. 9.

In Fig. 9a, as the solar multiple increases, the overall cost decreases. When the TSS capacity is 8 h and the solar multiple increases from 1.0 to 2.0, the overall cost decreases by approximately 15.68%. In Fig. 9b, the carbon emissions are also inversely proportional to the solar multiple. When the TSS capacity is 8 h and the solar multiple increases from 1.0 to 2.0, the carbon emissions decrease by approximately 16.98%. In Fig. 9c, when the TSS capacity is 8 h, the phenomenon of light abandonment occurs when the solar multiple is greater than 2.0, and at this time, PTPP is limited by the PB module capacity.

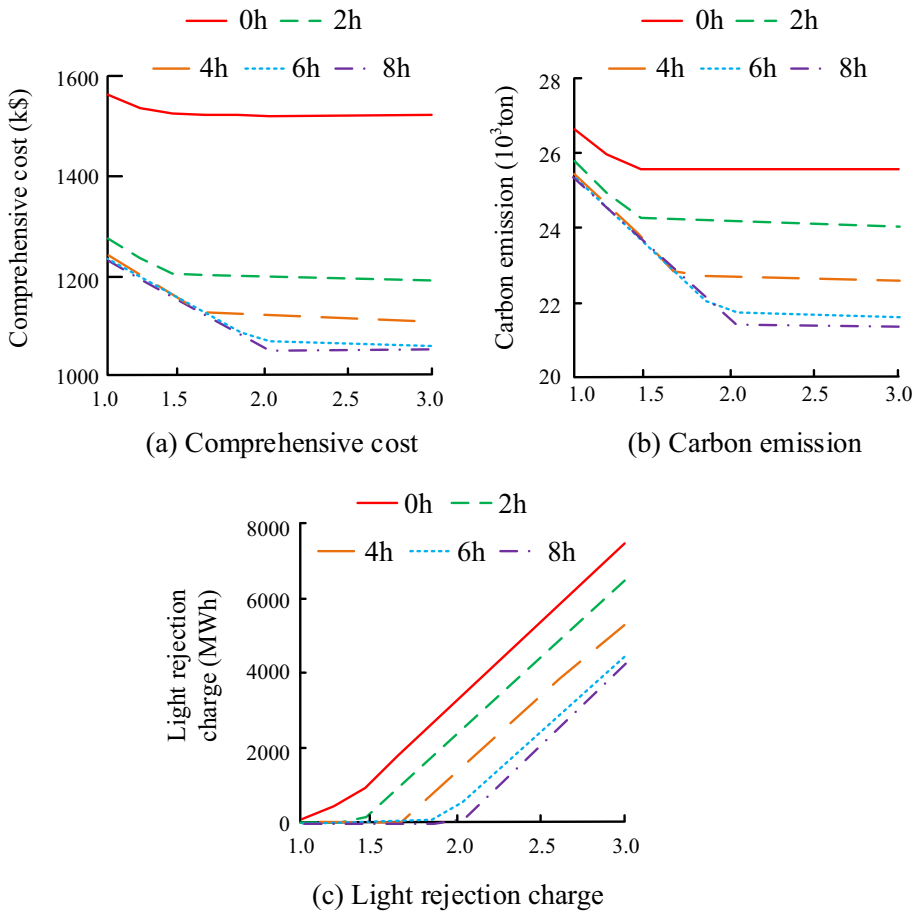

Fig. 9 Scheduling results of solar-thermal power station under solar multiple change

Discussions

Compared with the existing literature, Schöniger et al. (2021) also discussed the application of thermal energy storage in solar power generation, but this study conducted a more in-depth analysis and model construction on this basis, not only focusing on the overall performance of PTPP, but also going deep into the energy flow and conversion process within PTPP. TSS and other components of the solar thermal power plant (such as SF and PB) are integrated into a unified model, and advanced optimization algorithms and objective functions are used to build the model. In the simulation analysis, specific data on the impact of TES capacity on PTPP economy and carbon emission were shown, which provided empirical support for the integrated thermal energy storage and photothermal power generation scheme proposed by Kunwer et al. (2022).

While the model proposed in the study shows positive economic benefits and carbon reduction potential, there are limitations in scope and depth. First of all, the research mainly focuses on the design and optimization of the model, and does not fully explore the economic dynamics in different market and policy environments, such as electricity price fluctuations, subsidy policy changes, and competition in the renewable energy market, which may significantly affect the actual economic benefits of the model. In addition, although the model has achieved some results in reducing carbon emissions,

the environmental impact assessment is not comprehensive enough. The construction and operation of PTPP may have impacts on local biodiversity and water resource management that have not been fully explored in current research. The limitations of the model may limit its applicability under varying reality conditions. Simplified assumptions may lead to incomplete assessment of market fluctuations and environmental impacts, which in turn affects decision makers' judgment of project benefits. To improve model performance, future studies need to use more realistic assumptions, combine field tests and advanced technologies, and explore integration potential with other renewable energy sources.

At the implementation level, models may face issues such as technical challenges, infrastructure needs, high investment costs, and policy barriers. To ensure the practical feasibility of the model, it is recommended to strengthen technology research and development, promote infrastructure upgrades, explore innovative financing strategies, and work with policymakers to develop supportive policies. At the same time, a multi-stakeholder communication and cooperation mechanism will be established to jointly promote the implementation of the project and ensure that the model can take into account economic, technological and environmental factors to achieve the development of sustainable energy systems. In view of the increasing convergence of renewable energy technologies, the coexistence and optimization strategies of the proposed models with other renewable energy systems should be explored in the future. Through the integration of hybrid systems, the complementarity between different energy sources is utilized to improve the stability and reliability of the overall energy supply, while optimizing operations through intelligent scheduling and energy management strategies to contribute to a low-carbon and sustainable energy future.

Conclusion

In response to the high schedulability of PPG, this study proposed a self-running LCSO model for IEFCs considering PTPP. The construction process of the self-running model analyzed the energy conversion characteristics and coupling relationships of each energy module. The LCSO model was built on the basis of a self-running model, and finally an example analysis was conducted on the model. The simulation results of the self-running model showed that when the TSS capacity was 0 h, the IPGP of scheme AI and scheme BI were 31,577 $ and 9213 $, respectively. When the TSS capacity was 6 h, the IPGP of both AI and BI decreased to 0 $. As the capacity of the thermal storage module increased from 0 to 6 h, the power generation revenue of scheme AII increased from 34,830 to 64,409 $, and scheme BII increased from 54,240 $ to 62,251.9 $. The simulation of the LCSO model showed that when the TSS capacity increased from 0 to 8 h, the comprehensive operating cost decreased from 1635.2 k $ to 1224.6 k $, and the carbon emissions decreased from 26.4×10^3 ton to 22.1×10^3 ton. In addition, when the TSS capacity was 8 h, the phenomenon of light abandonment would occur when the solar multiple was greater than 2.0. At this time, PB module coordination was needed to achieve greater benefits. The research results indicate that the presence of TSS can effectively improve the power generation capacity of nighttime PTPP, which is beneficial for meeting the power generation plan and increasing the revenue of PTPP. This study provides theoretical guidance for the design and operation of PTPP, and has practical

significance for promoting the development of clean energy. In addition, for practitioners and decision-makers of PTPP, the study recommends that attention be paid to the research and development and optimization of TES, the formulation of supportive policies to promote technological innovation and investment, while paying attention to environmental protection and social benefits, through cross-field cooperation and long-term planning, jointly promote the development of PPG, to achieve a low-carbon transformation of the energy structure.

Abbreviations

PTPP	Photo thermal power plant
PPG	Photo thermal power generation
PVPP	Photovoltaic power plants
TSS	Thermal storage system
IEFC	Internal energy flow characteristics
LCSO	Low-carbon scheduling optimization
SF	Solar field
PB	Power block
HTS	Heat transfer system
M1	Heat collection–heat storage
M2	Heat collection–heat storage–power generation
M3	Heat collection–power generation
M4	Heat collection–heat releasing–power generation
M5	Heat releasing–power generation
M6	All idle
Scenario A	Applicable to the evening peak load network scenario
Scenario B	Applicable to the midday peak load network scenario
IPDP	Insufficient power generation

Author contributions
Jing Sun make all the contributions in this research.

Funding
Not applicable.

Availability of data and materials
All data and materials are within this article.

Declarations

Ethics approval and consent to participate
Not applicable.

Consent for publication
Not applicable.

Competing interests
There's no competing interests in this research.

Received: 15 March 2024 Accepted: 10 April 2024
Published online: 24 April 2024

References

Bloomfield HC, Brayshaw DJ, Gonzalez PLM, Charlton-Perez A (2021) Sub-seasonal forecasts of demand and wind power and solar power generation for 28 European countries. Earth Syst Sci Data 13(5):2259–2274
Buendía-Martínez F, Fernández-García A, Sutter F, Martinez-Arcos L, Reche-Navarro TJ, García-Segura A, Valenzuela L (2020) Uncertainty study of reflectance measurements for concentrating solar reflectors. IEEE Trans Instrum Meas 69(9):7218–7232
Carley S, Konisky DM (2020) The justice and equity implications of the clean energy transition. Nat Energy 5(8):569–577
Ding W, Bauer T (2021) Progress in research and development of molten chloride salt technology for next generation concentrated solar power plants. Engineering 7(3):334–347
Fang Y, Zhao S, Du E, Li S, Li Z (2021) Coordinated operation of concentrating solar power plant and wind farm for frequency regulation. J Modern Power Syst Clean Energy 9(4):751–759
Frizzo Stefenon S, Kasburg C, Nied A, Rodrigues Klaar AC, Silva Ferreir FC, Waldrigues Branco N (2020) Hybrid deep learning for power generation forecasting in active solar trackers. IET Gener Transm Distrib 14(23):5667–5674

Guerra OJ, Zhang J, Eichman J, Denholm P, Kurtz J, Hodge BM (2020) The value of seasonal energy storage technologies for the integration of wind and solar power. Energy Environ Sci 13(7):1909–1922
Hamilton WT, Husted MA, Newman AM, Braun RJ, Wagner MJ (2020) Dispatch optimization of concentrating solar power with utility-scale photovoltaics. Optim Eng 21(1):335–369
Haruna AA, Muhammad LJ, Abubakar M (2023) Novel thermal-aware green scheduling in grid environment. Artif Intell Appl 1(4):244–251
Hou X, Wild M, Folini D, Kazadzis S, Wohland J (2021) Climate change impacts on solar power generation and its spatial variability in Europe based on CMIP6. Earth Syst Dyn 12(4):1099–1113
Khaloie H, Vallée F, Lai CS, Toubeau JF, Hatziargyriou ND (2021) Day-ahead and intraday dispatch of an integrated biomass-concentrated solar system: a multi-objective risk-controlling approach. IEEE Trans Power Syst 37(1):701–714
Kunwer R, Pandey S, Pandey G (2022) Technical challenges and their solutions for integration of sensible thermal energy storage with concentrated solar power applications—a review. Process Integr Optim Sustain 6(3):559–585
Manoharan P, Subramaniam U, Babu TS, Padmanaban S, Holm-Nielsen JB, Mitolo M, Ravichandran S (2020) Improved perturb and observation maximum power point tracking technique for solar photovoltaic power generation systems. IEEE Syst J 15(2):3024–3035
Palacios A, Barreneche C, Navarro ME, Ding Y (2020) Thermal energy storage technologies for concentrated solar power—a review from a materials perspective. Renew Energy 156(1):1244–1265
Schöniger F, Thonig R, Resch G, Lilliestam J (2021) Making the sun shine at night: comparing the cost of dispatchable concentrating solar power and photovoltaics with storage. Energy Sources Part B 16(1):55–74
Shakya S (2021) A self-monitoring and analyzing system for solar power station using IoT and data mining algorithms. J Soft Comput Paradigm 3(2):96–109
Wang Q, Hobbs WB, Tuohy A, Bello M, Ault DJ (2021) Evaluating potential benefits of flexible solar power generation in the southern company system. IEEE J Photovolt 12(1):152–160
Yousef BAA, Hachicha AA, Rodriguez I, Abdelkareem MA, Inyaat A (2021) Perspective on integration of concentrated solar power plants. Int J Low-Carbon Technol 16(3):1098–1125
Yu D, Ebadi AG, Jermsittiparsert K, Jabarullah NH, Vasiljeva MV, Nojavan S (2020) Risk-constrained stochastic optimization of a concentrating solar power plant. IEEE Trans Sustain Energy 11(3):1464–1472

Publisher's Note